

RESEARCH

Open Access



Frequency estimation for underwater CW pulse by interpolation on fractional Fourier coefficients based on amplitude ratio method

Lin Li^{1,2,3}, JingWei Yin^{1,2,3}, Xiao Han^{1,2,3*} and Wei Ge^{1,2,3}

*Correspondence:
hanxiao1322@hrbeu.edu.cn

¹ Acoustic Science
and Technology Laboratory,
Harbin Engineering University,
Harbin 150001, China

² Key Laboratory of Marine
Information Acquisition
and Security (Harbin Engineering
University), Ministry of Industry
and Information Technology,
Harbin 150001, China

³ College of Underwater Acoustic
Engineering, Harbin Engineering
University, Harbin 150001, China

Abstract

Fast and accurate estimation of sinusoidal signals plays an important role in many fields like communications, radar, sonar, etc. In underwater signal processing applications, sinusoidal signals usually take the form of CW pulses in most practical applications, therefore, zero-padding and duty-cycle show their great importance to the estimation of sinusoidal signals. In this paper, a high-precision estimation algorithm of sinusoidal signal is proposed, which combines amplitude ratio algorithm and fractional Fourier coefficient interpolation algorithm. The proposed algorithm uses the adjacent spectral line ratio algorithm instead of the Fourier coefficient maximum amplitude discrete spectral line search algorithm for coarse estimation, and modifies the traditional interpolation method. The proposed algorithm improves the Fourier coefficient interpolation algorithm by combining zero-padded signals to achieve the accurate frequency estimation for zero-padded sinusoidal signal. The performance of the algorithm is also in accordance with theoretical level for zero-padded signals, which is a great improvement over the frequency estimation algorithm for non-padded signals as well as the algorithm for zero-padding signals. The theoretical results are verified by extensive computer simulations which show that the proposed algorithm can both achieve better results for zero-padding cases and maintain comparable performance with competing algorithms for the non-padded signal. Therefore, the algorithm can be better applied to practical underwater detection or communication signals.

Keywords: Frequency estimation, DFT interpolation, Underwater signal processing, CW pulse, Zero-padding

1 Introduction

Accurate estimation of a sinusoidal frequency signal at low signal-to-noise ratio has been a fundamental issue in many fields such as digital signal processing, sonar, communications, and radar [1, 2]. In underwater signal processing, the limitations of the speed of sound are more sensitive to relative motion, resulting in much larger frequency shifts as well as Doppler than on land. And in the field of underwater signal processing, the impact of this frequency shift is often not negligible [3]. Accurate parameter estimation of signals can be obtained by accurate estimation of frequency, which is important for synchronization in signal processing, for frequency compensation and for other

issues. The commonly used methods for frequency estimation include time domain method, frequency domain method, maximum likelihood method, and eigen-subspace method [4, 5]. The time domain method is computationally small and obviously disadvantageous under low signal-to-noise ratio conditions, but it has low accuracy, and requires high signal-to-noise ratio. The probability class methods, such as maximum likelihood method, are computationally large and mean little to the estimation of a single parameter, while the subspace class methods are mostly used for the estimation of multi-sinusoidal signals. Therefore, the study of single-sinusoidal signals adopts mainly frequency-domain methods, whereby the frequencies estimate will be divided into two steps: coarse estimation based on FFT is firstly performed, and then the residual frequency deviation using interpolation iterations is estimated. Rife algorithm [6, 7] is a classical amplitude ratio interpolation algorithm based on the maximum spectral coefficient of Fourier coefficients. Proposed by Rife in 1970, the algorithm is a classical integer interpolation algorithm, detailed principles of which will be briefly introduced below. Though the method is so easy and applicable that it can be regarded as the originator of various subsequent interpolation class algorithms, it limits the residual frequency deviation and is easily affected by noise. To solve the problem, Modified Rife Algorithm (MRife) was proposed [8, 9]. The improvement in MRife is to focus on higher accuracy of Rife algorithm when $|\delta|=0.5$, and then the process is as follows: First, the reference interval $[1/3, 1/2]$ is set, and then it is estimated to obtain $\hat{\delta}$. If $\hat{\delta}$ within the interval, the estimation is considered correct; and if it is not within this interval, the sinusoidal signal is shifted by $1/3$ units, and then X_l and X_0 is recalculated according to the estimation formula of $\hat{\delta}$. These steps were performed iteratively and the final estimate is completed minus the compensated frequency shift. This method reduces the defects of large errors with the Rife algorithm but does not fundamentally solve the problem of poor performance of the Rife algorithm at low signal-to-noise ratios. Inspired by the Modified Rife Algorithm, some fractional interpolation algorithms, as well as fractional square interpolation algorithms, have been proposed one after another, which improves accuracy of the interpolation algorithm estimated results. These algorithms include FFCI algorithm, MOI algorithm [10], etc. But as long as we adopt the interpolation algorithm, we need to face its fatal defects, that is, it is very sensitive to the coarse estimation results. The traditional interpolation algorithm is on the basis of the MBS algorithm which is the most basic FFT search algorithm, which means no matter how to fix it, it is always going to have better effects within a certain range. For example, with the classical FFCI algorithm, better effects only can be obtained when δ is close to 0, with MMSE close to 1.0147 times the CRLB.

Following this way, Aboutanios and Mulgrew proposed the well-known AM frequency estimation algorithm in 2005, which adds iterative steps to the fractional interpolation class algorithm so that the defects are well corrected, which refer to the bad effects of the FFCI algorithm and the MOI algorithm when the deviation of initial estimate is large. These two algorithms are the two iteration of the AM algorithm [11]. In recent years, more advanced iterative frequency estimation algorithms have been proposed [12, 13]. In 2017 [14] Ye S and Aboutanios et al. suggested an iterative frequency estimation algorithm based on the AM algorithm, which can estimate not only the frequency but also the initial phase and the amplitude of signals. In 2018, Serbes proposed a QSE algorithm

for interpolating the q -shifted DFT coefficients of signals and a HAQSE algorithm using a hybrid half-shifted and q -shifted DFT interpolator, which is still essentially an iterative FFT coefficient interpolation algorithm [15]. In essence, these types of interpolating estimators are finding the solution of a nonlinear equation. In order to allow a better understanding of the estimate bias of these estimators and to explain why some interpolation estimators perform better than others, Liao J R [16] introduced a new set of unbiased estimators using analytical solutions. Candan proposed in his articles [17–19] a series of estimation methods of frequency and offered a fast estimation method by table lookup, which can save more computational effort. But it can be found in the simulation that the residual bias of the method still has some influence on the estimation results with few iterations. In summary, by comparison of simulations, it can be found that the estimation methods of QSE and HAQSE proposed by Serbes are by far the best methods for estimation accuracy of single-sinusoidal signal. In paper [20], further investigation on DFT interpolation is carried out to examine some issues that are still open. They start by evaluating the Cramér–Rao bound (CRB) for frequency recovery by interpolation of two q -shifted 16 spectral lines and assess its dependence on ϵ and q , however, they does not discuss the theoretical error in the zero-padding case.

All the algorithms mentioned previously are for non-padded signals. Then the following studies are for zero-padded signals by some scholars. RCTSL algorithm [21] was proposed in 2011, which was a method for estimating accurately the signal frequency even at low signal-to-noise ratio without iterative computation. The main concept of it is to calculate the error of the power spectrum and the square of the signal DFT transform result, for the frequency is closest to the true frequency value when the square of the interpolation of the two is smallest, so that the frequency estimation is converted into a basic concept of optimization, for which a closed-form solution can be obtained by derivation. The article pointed out that the method had the folk-singing advantages: it is highly accurate; the calculation is simple; and iterative calculation is not needed. The algorithm provokes the thought for the conventional FFT difference algorithm, which is of valuable reference. The algorithm is also deserving praise because it can be used effectively for zero-padded signals. But it is regretful to say that these algorithms [22, 23] work only when the signal length is an integer multiple of the sinusoidal signal, but does not work effectively for non-integer multiple interpolation. In 2016, an accurate frequency estimation scheme [24] based on zero-padded signals was proposed, which took the maximum likelihood estimation as a coarse estimate and used FFT coefficient interpolation as an accurate estimate. But it is a regret that the simulation performance of the method is not superior, and the theoretical error of the method is not further indicated. In 2021, Yixiong Zhang et al. proposed an ARD frequency estimation algorithm [25] for adjacent spectral lines based on the maximum spectral lines, which estimated the value using the ratio of the maximum spectral lines to adjacent spectral lines, thus the estimation of the accurate single frequency signal was performed. Relative to RCTSL algorithm, ARD algorithm does not for finding a closed solution, instead, the monotone function is used to approximate the ratio function in a certain range based on Newton gradient descent method. By this way, the algorithm is more adaptable to signals with different zero-padding and duty-cycle, but, it also has higher complexity. Relatively,

the method has higher accuracy compared to the RCTSL algorithm, and it has also better results for estimating zero-padded signals after improvement in zero-padding. However, the algorithm is the result of approximation by Newton's method, hence the performance of the algorithm cannot be accurately obtained except for simulation. Moreover, the method does not give the theoretical estimation error. Nevertheless, the algorithm is still the best estimation method that can be found for the estimation results of zero-padded signals.

In this paper, the authors propose an accurate frequency estimation algorithm based on modified Amplitude Ratio of DFT coefficient (ARD) algorithm and modified Fractional Fourier coefficient interpolation (FFCI) algorithm. The existing problem in the calculation of all FFT interpolation class algorithms is that traditional frequency interpolation algorithm is not effective because it is sensitive to the coarse estimation results. The proposed algorithm in this paper combines with ARD algorithm for frequency coarse estimation, which makes the residual frequency deviation close to 0. In this way, compared with AM algorithm, this algorithm can achieve good estimation results without iteration and is not inferior to some advanced frequency estimation algorithms, such as the QSE proposed in recent years. The interpolation algorithm based on zero-padded signals is improved further and the performance of the improved interpolation algorithm is derived theoretically in this paper. Compared to other algorithms, the algorithm proposed in this paper can not only achieve the frequency estimation close to CRLB under the condition of non-padded signal, but also make an accurate estimation of zero-padded signals. The asymptotic CRLB for the zero-padded signal was derived and it fits well with the simulation results. Due to multiple iterations, the algorithm proposed in this paper has the drawback of large computation, but for frequency estimation, the real-time requirement is not very high. Moreover, the current DSP processor has higher performance than iterative decoding, and due to fast and efficient FFT computation, iterative frequency estimation can be attainable in practical applications.

The outline of this paper is as follows: firstly a general theoretical basis of the interpolation class algorithm will be introduced, then we carry out the derivation of the coarse estimation based on the amplitude ratio method and the derivation of the improved fractional Fourier coefficient interpolation method for the zero-padded signal. Thirdly, the theoretical performance of the method will be estimated, and finally the verification in a large number of numerical simulations is presented.

2 Theoretical basis of frequency estimation based on frequency domain interpolation

The core concept of the frequency domain method is to interpolate the FFT coefficients so as to continuously approximate the true frequency value. One of the two typical categories is the iterative difference algorithm based on the FFT coefficients, which represented by the Rife [6] algorithm and the AM [11] algorithm. The other type is ratio of interpolation algorithm on the basis of the ratio of the spectral power between the adjacent spectral lines and the maximum spectral line, which is represented by the ARD [25] algorithm. The detailed introduction is as follows.

First, we assume a sinusoidal signal is expressed as follows:

$$s(n) = Ae^{j\left(2\pi f_0 T_s \left(n - \frac{N}{2}\right) + \theta\right)}, n = 0, \dots, N-1 \quad (1)$$

$$r(n) = s(n) + w(n). \quad (2)$$

where A , f and θ are the amplitude, frequency, and initial phase, respectively, and T_s is the sampling interval, and the noise is Gaussian white noise with a mean of 0 and variance of σ^2 . According to the definition mentioned previously, we can obtain the signal-to-noise ratio as $SNR = A^2/\sigma^2$, the sampling frequency as $f_s = 1/T_s$. When the sinusoidal signal amplitude, frequency and initial phase are unknown, the Cramer lower bound (CRLB) for the full-band estimation of the great likelihood estimation of the sinusoidal signal was proposed in the literature [26],

$$\sigma_f^2 = \frac{6f_s^2}{(2\pi)^2 \cdot SNR \cdot N(N^2 - 1)}. \quad (3)$$

When N is much greater than 1,

$$\sigma_f^2 \approx \frac{6f_s^2}{(2\pi)^2 \cdot SNR \cdot N^3}. \quad (4)$$

Generally, we adopt the MSE for estimation error to measure the accuracy of a frequency estimation method. For CRLB being proposed, the ratio of MSE/CRLB is used to evaluate the accuracy of an estimation method when performing frequency estimation.

When performing the FFT, the minimum distinguishable frequency interval is $\Delta f = f_s/N$, where N is the number of FFT points, and assuming that the spectral line where we obtain the spectral peak is the m^{th} , the FFT coarse estimation of the frequency value can be obtained as $\hat{f}_0 = \Delta f \times m$. However, as shown in Fig. 1, in most

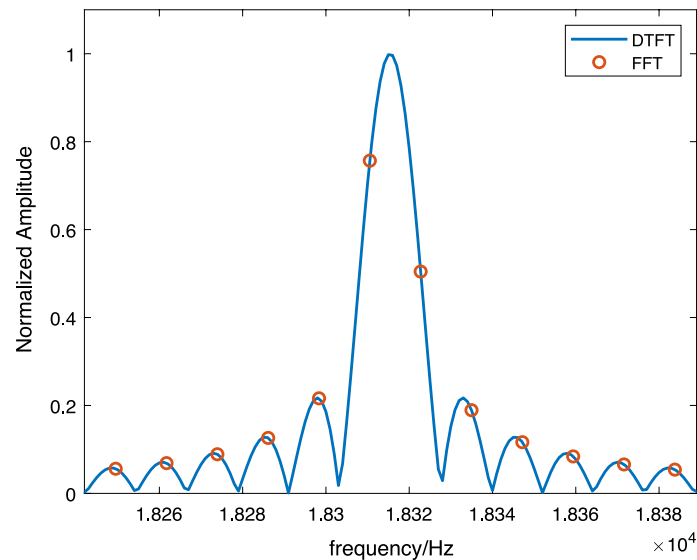


Fig. 1 Comparison of DFT and FFT coefficients in the presence of bias in practice

cases, the FFT estimation has a frequency deviation unless the peak happens to be at the sampling point, the size of which depends on the size of FFT points and sampling rate. The reason is that the discrete sampling is in the frequency domain, there is bound to be a deviation from the estimated FFT peak to the true peak. Assuming that the frequency deviation factor is δ , the purpose of our accurate frequency estimation is to find this residual deviation, so as to find an accurate frequency estimation result of $f = \Delta f \times (m + \delta)$, where $\delta \in [-0.5, 0.5]$. If δ is greater than $+0.5$, the FFT coarse estimate maximum should be $m+1$, similarly, the estimate should be $m-1$ when δ is less than -0.5 .

So, when we estimate the frequency, the DFT value X_l with a spectral peak spectral line at distance l was firstly calculated,

$$X_l = \sum_{n=0}^{N-1} r(n) \exp(-j2\pi n(m+l)/N). \quad (5)$$

Combining Eqs. (1) and (2) and the results of frequency estimation mentioned before, we can obtain:

$$X_l = A \exp(j\theta) \times \frac{1 - \exp(j2\pi(\delta - l))}{1 - \exp(j2\pi(\delta - l)/N)} + W_l. \quad (6)$$

Usually, for $2\pi(\delta - l)/N \ll 1$, we replace the denominator part of Eq. (6) with the equivalent infinitesimal $j2\pi(\delta - l)/N$, which eventually leads to writing X_l as

$$X_l = \frac{NA \exp(j\theta)}{j2\pi} \times \frac{\exp(j2\pi\delta) \cdot \exp(-j2\pi l) - 1}{(\delta - l)} + W_l. \quad (7)$$

This is the base model for our later discussion of complex sinusoidal signals. The main idea of Rife algorithm [6] is to let l be 0 or ± 1 , and so we can write Eq. (7) as

$$X_l = \frac{\delta}{\delta - l} NA \text{sinc}(\pi\delta) \exp(j(\pi\delta + \theta)) + W_l. \quad (8)$$

Disregarding the noise spectrum, so that

$$\alpha = \frac{|X_l|}{|X_0|} = \left| \frac{\delta}{\delta - l} \right| = \begin{cases} \frac{\delta}{1-\delta}, & l = 1 \text{ and } \delta > 0 \\ \frac{-\delta}{1-\delta}, & l = -1 \text{ and } \delta < 0 \end{cases}. \quad (9)$$

So, we can obtain $\hat{\delta}$ and the final frequency estimate \hat{f} as follows

$$\hat{\delta} = \frac{\alpha}{1+\alpha} = \frac{|X_l|/|X_0|}{1 + |X_l|/|X_0|}, \quad (10)$$

$$\hat{f} = \Delta f (m + l \cdot \hat{\delta}). \quad (11)$$

Obviously, this allows us to obtain an estimate of δ from observations of the value of α , which can be obtained from Eq. (7).

The AM algorithm [11] was proposed by Aboutanios and Mulgrew in 2005. The main concept is to frequency shift the signal, constantly approaching the point where

the frequency deviation is zero and estimating the residual. Only two Fourier coefficients $X_{+0.5}$ and $X_{-0.5}$ were used for cycling interpolation. Observing Eq. (8) and letting $l = \pm 0.5$, it can be organized as

$$X_l = \frac{\delta}{\delta - l} NA \frac{\cos(\pi \delta)}{\pi \delta} \exp(j(\theta + \pi \delta + \pi/2)) + W_l, \quad (12)$$

$$2\delta = \frac{X_{0.5} + X_{-0.5}}{X_{0.5} - X_{-0.5}}. \quad (13)$$

According to the theory, the performance of this interpolation algorithm is poor when the residual is close to ± 0.5 for one operation, though it can be very close to the CRLB when the residual frequency is close to zero. The AM algorithm adds an iteration step to this process, that is, it hopes to reduce the residual error by the previous iteration estimation, so that the later iteration process can be considered to have a residual error close to 0. The simulation shows that such a strategy works well, and only two iterations are needed to achieve good results.

3 The accurate frequency estimator based on sinusoidal signals with zero-padding

3.1 Sinusoidal signal with zero-padding in underwater case

In the previous section we briefly introduced the theoretical basis of frequency domain interpolation, however, in the process of underwater signal processing, sinusoidal signals are often in the form of CW pulses. We give two examples of the application of sinusoidal signals in underwater acoustic signal processing in Fig. 2. Figure 2a shows an application in communications, where we superimpose a low power CW pulse on the signal of data and pilot, the relationship between this signal and the communications signal is superimposed in the time domain and does not overlap in the frequency domain, as the single frequency signal occupies very little bandwidth, so the frequency estimation signal occupies very little

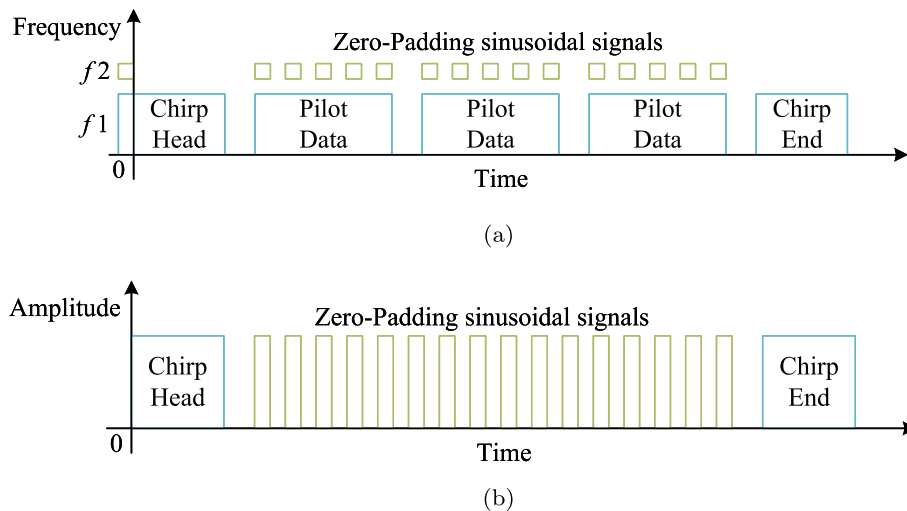


Fig. 2 Application scenarios for sinusoidal pulses in underwater signal, **a** Application in underwater acoustic communication signals, **b** Applications in underwater acoustic detection signals

bandwidth resources. Figure 2b then shows the application in the detection signal. It is worth noting that during underwater sound propagation, the effects of relative motion are much more dramatic than on land due to the slower speed of sound, so we add a Chirp signal before and after the signal as a synchronization, in practice a hyperbolic FM signal with Doppler invariance can be used, so that the compression and expansion of the whole frame due to the larger Doppler can be compensated for first by the synchronization signal, then the frequency estimation algorithm is performed. As the Doppler before and after the pulse can be inconsistent, we capture and process the CW pulse signal one pulse period at a time.

3.2 Sinusoidal signal model with zero-padding

Based on the assumption of zero-padding of the signal, we propose the following signal model, where M is the total length of the signal and N is the length of the nonzero part

$$\tilde{s}(n) = \begin{cases} s(n), & 0 \leq n \leq N-1 \\ 0, & N \leq n \leq M-1 \end{cases} \quad (14)$$

$$\tilde{r}(n) = \begin{cases} r(n), & 0 \leq n \leq N-1 \\ 0, & N \leq n \leq M-1 \end{cases} \quad (15)$$

$$f_0 = (p+x) \cdot \Delta f = (p+x) \cdot \frac{F_s}{M}, \quad (16)$$

where $|x| \leq 0.5$, so that the form of the received signal can be obtained as follows,

$$\tilde{R}(k) = \sum_{n=0}^{N-1} \tilde{r}(n) e^{-j2\pi k \frac{n}{M}} = \tilde{S}(k) + \tilde{W}(k), \quad k = 0, 1, \dots, M-1, \quad (17)$$

$$\begin{aligned} \tilde{S}(k) &= A \sum_{n=0}^{N-1} e^{j\left(2\pi(p+x)\frac{F_s}{M}\left(n-\frac{M}{2}\right) \cdot T_s + \theta\right)} e^{j2\pi k \frac{n}{M}} \\ &= A e^{j\theta} e^{-j\pi(p+x)} \sum_{n=0}^{N-1} e^{j2\pi(p+x-k)\frac{n}{M}}. \end{aligned} \quad (18)$$

3.3 Coarse estimation of frequency based on amplitude ratio method

The signal is analyzed firstly ignoring the effect of noise. The FFT estimation results for a single frequency signal with zero-padding can be written as

$$\begin{aligned} \tilde{S}(p) &= A e^{j\theta} e^{-j\pi(p+x)} \sum_{n=0}^{N-1} e^{j2\pi x \frac{n}{M}} \\ &= \frac{A \sin\left(\frac{\pi x N}{M}\right)}{\sin\left(\frac{\pi x}{M}\right)} e^{j\pi x \frac{N-1}{M}} e^{j\theta} e^{-j\pi(p+x)}. \end{aligned} \quad (19)$$

Sort out the terms that are independent of p , let $\phi = \theta + \pi x(N-1)/(M-1)$, which is a constant value in the effect for the FFT coefficients, and then further simplify the above equation to

$$\tilde{S}(p) = \frac{A \sin\left(\frac{\pi x N}{M}\right)}{\sin\left(\frac{\pi x}{M}\right)} e^{j\phi} e^{-j\pi p}. \quad (20)$$

Here the p we are looking for is the index of the FFT coefficients, so it is an integer, then the following equation can be obtained

$$e^{-j\pi p} = \begin{cases} 1 & p \text{ is even} \\ -1 & p \text{ is odd.} \end{cases} \quad (21)$$

Then, according to the above equation, adjacent FFT coefficients are, respectively:

$$\tilde{S}(p+1) = \frac{A \sin\left(\pi \frac{x-1}{M} N\right)}{\sin\left(\pi \frac{x-1}{M}\right)} e^{j\phi} e^{-j\pi\left(p+\frac{N-1}{M}\right)}, \quad (22)$$

$$\tilde{S}(p-1) = \frac{A \sin\left(\pi \frac{x+1}{M} N\right)}{\sin\left(\pi \frac{x+1}{M}\right)} e^{j\phi} e^{-j\pi\left(p-\frac{N-1}{M}\right)}. \quad (23)$$

It can be noted that the FFT coefficients adjacent to the signal peak coefficients are easily accessible. According to Eqs. (22) and (23), we can obtain

$$g(x) = \begin{cases} \frac{|\tilde{S}(p-1)|}{|\tilde{S}(p)|} = g_l(x), & -0.5 < x < 0, \\ \frac{|\tilde{S}(p+1)|}{|\tilde{S}(p)|} = g_r(x), & 0 < x < 0.5. \end{cases} \quad (24)$$

Then, two different ratio functions for the two intervals can be obtained, respectively.

$$g_l(x) = \frac{\sin\left(\pi \frac{x}{M}\right)}{\sin\left(\pi \frac{xN}{M}\right)} \cdot \frac{\sin\left(\pi \frac{1+x}{M} N\right)}{\sin\left(\pi \frac{1+x}{M}\right)}, \quad -0.5 < x < 0. \quad (25)$$

$$g_r(x) = \frac{\sin\left(\pi \frac{x}{M}\right)}{\sin\left(\pi \frac{xN}{M}\right)} \cdot \frac{\sin\left(\pi \frac{1-x}{M} N\right)}{\sin\left(\pi \frac{1-x}{M}\right)}, \quad 0 < x < 0.5. \quad (26)$$

We can obtain the FFT coefficients of the signal from the received signals easily.

$$\tilde{R}(p) = \tilde{S}(p) + \tilde{W}(p), \quad (27)$$

$$\tilde{R}(p-1) = \tilde{S}(p-1) + \tilde{W}(p-1), \quad (28)$$

$$\tilde{R}(p+1) = \tilde{S}(p+1) + \tilde{W}(p+1). \quad (29)$$

Since the power of Gaussian white noise is almost the same at all frequency points, we assume that the value of is the same at all frequency points. Another assumption is that

the SNR of the signal is known, so we assume it as a constant related to the SNR as a correction term, thus our problem is converted into finding the solution of the following two equations:

$$\frac{\tilde{R}(p-1) - W}{\tilde{R}(p) - W} = \frac{\sin\left(\pi \frac{x}{M}\right)}{\sin\left(\pi \frac{xN}{M}\right)} \cdot \frac{\sin\left(\pi \frac{1+x}{M}N\right)}{\sin\left(\pi \frac{1+x}{M}\right)}, -0.5 < x < 0, \quad (30)$$

$$\frac{\tilde{R}(p+1) - W}{\tilde{R}(p) - W} = \frac{\sin\left(\pi \frac{x}{M}\right)}{\sin\left(\pi \frac{xN}{M}\right)} \cdot \frac{\sin\left(\pi \frac{1-x}{M}N\right)}{\sin\left(\pi \frac{1-x}{M}\right)}, 0 < x < 0.5. \quad (31)$$

However, it is difficult to obtain a closed-form solution of the above equation because it is not a linear equation. But it can be noticed from Fig. 3 that $g(x)$ is monotonically decreasing when $-0.5 < x < 0$. Meanwhile the function is monotonically increasing when $0 < x < 0.5$. In the corresponding interval, according to the function has the property of monotonically increasing or monotonically decreasing, we can use Newton's gradient descent method to find the solution for the corresponding value. However, the above equation is not a linear equation, to obtain a closed-form solution of the above equation is more difficult, but according to Fig. 3 we can notice that, according to Fig. 3, we can see that when $-0.5 < x < 0$, $g(x)$ is monotonically decreasing, and when $0 < x < 0.5$. In the corresponding intervals, Newton's gradient descent method can be used to find the solution for the corresponding value, considering the function properties of monotonically increasing or decreasing.

Our point then was shifted to how to obtain the corresponding function value and the corresponding function, that is, how to determine whether the true value is to the left or to the right of the peak.

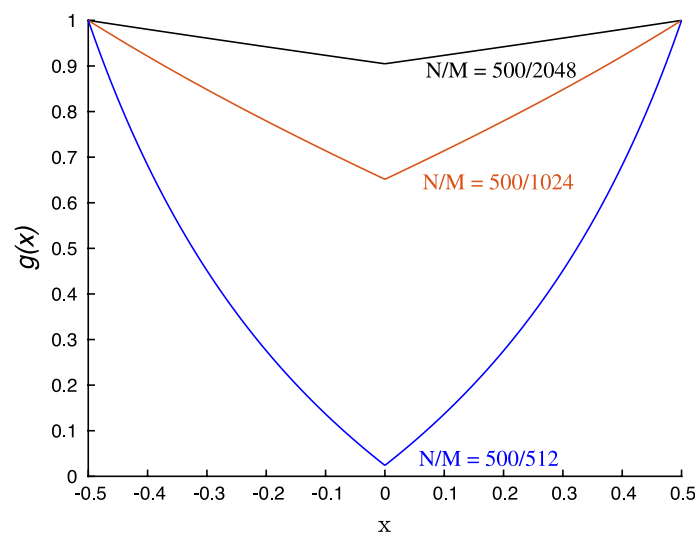


Fig. 3 Schematic diagram of $g_l(x)g_r(x)$ with several different parameters

It can be seen from Fig. 4 that whether the true value is to the left or right of the peak, we can assume that the true frequency point is between the maximum FFT coefficient point and the second point. Assume that two different x values can be obtained from the two intervals, respectively, and then bring them to Eqs. (30) and (31) to obtain the corresponding x_r or x_l . All we need to do is to calculate the value of x from the $g(x)$ value obtained by the ratio. Obviously, a $g(x)$ corresponding to an x -solution is not unique, then we can obtain two x values accordingly: one at $(-0.5, 0)$ and one at $(0, 0.5)$. It is also natural to obtain two different frequency values f_r and f_l .

We then define according to DTFT,

$$D(f) = \sum_{n=0}^{N-1} \tilde{r}(n) e^{-j2\pi f n}, \quad 0 \leq f \leq F_s. \quad (32)$$

The frequency value was calculated and obtained, then we can calculate the DTFT value corresponding to the received signal. It can be seen from Fig. 4 that the true frequency value should be near the DTFT maximum. Thus, by size comparison between the two DTFT values, we can determine which direction the true frequency value fits better. Considering the calculated DTFT values after the comparison, it is concluded that the coarse estimate of the frequency is in its greater direction.

At this point, we have completed the coarse estimation of the received signals by using the amplitude ratio method.

3.4 Accurate estimation of frequency based on fractional Fourier coefficient interpolation

In the literature [11], precise estimate was performed with iterative interpolation at the distance A on both sides of the coarse estimate of the signal. It can be seen from the simulation that the coarse estimation is less enhanced by this estimation method for zero-padded signals. We then improve this method by combining zero-padded signals.

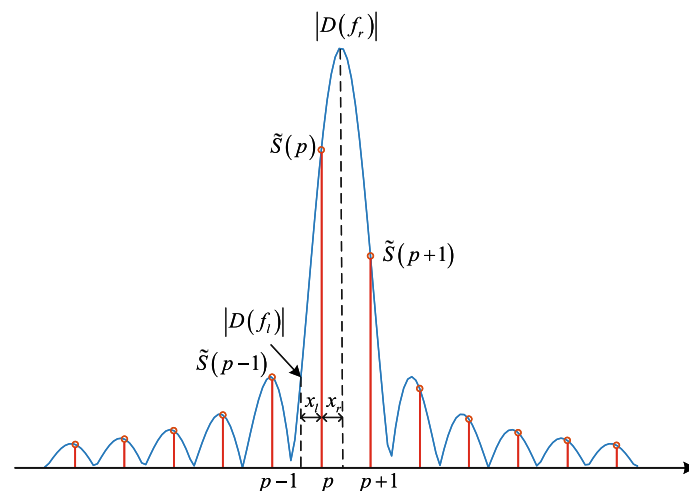


Fig. 4 Diagram showing the relationship between DTFT and DFT coefficients in the vicinity of the peak point

After the coarse estimate of the frequency was obtained by using the improved ratio method, the improved iterative FFT coefficient interpolation algorithm was applied to compensate the precise frequency estimation error of the signals.

$$f = \frac{\hat{m} + \delta}{M} f_s. \quad (33)$$

where \hat{m} is the coarse estimated DFT coefficient, which is $p + x_r$ or $p + x_l$ in the previous section, δ is the remaining residual. As mentioned before, in general, δ takes values in the range of $[-0.5, 0.5]$.

We first calculate the DFT coefficients at Δp on both sides of the coarse estimate \hat{m}

$$X_{\Delta p} = \sum_{k=0}^{M-1} s(k) e^{-j2\pi k \frac{\hat{m} + \Delta p}{M}} + W_{\Delta p}, \quad \Delta p = \pm 0.5 \frac{M}{N}. \quad (34)$$

According to the previous section, $s(k) = 0$ when k is greater than N . We take the value partially adjusted for zero-padding as follows

$$X_{\Delta p} = \sum_{k=0}^{N-1} s(k) e^{-j2\pi k \frac{\hat{m} + \Delta p}{M}} + W_{\Delta p}, \quad \Delta p = \pm 0.5 \frac{M}{N}. \quad (35)$$

Bring $s(k)$ into the above equation, and using the summation formula of the isometric series, we get:

$$\begin{aligned} X_{\Delta p} &= e^{j\theta} \frac{A_0 \left(1 - e^{-j2\pi \left(\frac{\Delta p - \delta}{M} \right) N} \right)}{1 - e^{-j2\pi \left(\frac{\Delta p - \delta}{M} \right)}} + W_{\Delta p}, \\ &= e^{j\theta} \frac{A_0 \left(1 - e^{-j2\pi \left(\Delta p \frac{N}{M} - \delta \frac{N}{M} \right)} \right)}{1 - e^{j2\pi \left(\frac{\delta - \Delta p}{M} \right)}} + W_{\Delta p}, \quad \Delta p = \pm 0.5 \frac{M}{N}. \end{aligned} \quad (36)$$

Since $\delta - \Delta p \ll M$, by the principle of equivalent infinitesimals, we can reduce Eq. (35) to:

$$\begin{aligned} X_{\Delta p} &= A_0 e^{j\theta} \frac{\left(1 - e^{-j2\pi \Delta p \frac{N}{M}} e^{j2\pi \delta \frac{N}{M}} \right)}{-j2\pi \frac{\delta - \Delta p}{M}} + W_{\Delta p} \\ &= -MA_0 e^{j\theta} \frac{\left(1 - e^{-j2\pi \Delta p \frac{N}{M}} e^{j2\pi \delta \frac{N}{M}} \right)}{j2\pi \delta} \frac{\delta}{\delta - \Delta p} + W_{\Delta p}. \end{aligned} \quad (37)$$

To make $-MA_0 e^{j\theta} \frac{\left(1 - e^{-j2\pi \Delta p \frac{N}{M}} e^{j2\pi \delta \frac{N}{M}} \right)}{j2\pi \delta}$ independent of Δp , we take $\Delta p = \pm 0.5 \frac{M}{N}$, and we can obtain:

$$\begin{aligned}
X_{\Delta p} &= -MA_0 e^{j\theta} \frac{(1 - e^{-j2\pi \Delta p \frac{N}{M}} e^{j2\pi \delta \frac{N}{M}})}{j2\pi \delta} \frac{\delta}{\delta - \Delta p} + W_{\Delta p} \\
&= MA_0 e^{j\theta} \frac{(1 + e^{j2\pi \delta \frac{N}{M}})}{j2\pi \delta} \frac{\delta}{\delta - \Delta p} + W_{\Delta p}, \Delta p = \pm 0.5 \frac{M}{N}.
\end{aligned} \quad (38)$$

Let $-MA_0 e^{j\theta} \frac{(1 + e^{j2\pi \delta \frac{N}{M}})}{j2\pi \delta}$ be b , then get:

$$X_{\Delta p} = b \frac{\delta}{\delta - \Delta p} + W_{\Delta p} \quad (39)$$

Since $\Delta p = \pm p = \pm 0.5 \frac{M}{N}$, neglecting the effect of noise, we obtain

$$\beta = \frac{X_p + X_{-p}}{X_p - X_{-p}} \doteq \frac{2N\delta}{M}. \quad (40)$$

3.5 Overall algorithm flow

Then accurate estimate of the residual frequency bias can be obtained. Combining coarse estimates with accurate estimates, the complete frequency estimation method is presented as follows:

Step1 : PerformFFTcalculationofMpoints

Firstly, an FFT calculation of the received signal at M points to obtain the maximum spectral level position, denoted as $R(p)$, and record its adjacent spectral coefficients $R(p-1)$, $R(p+1)$, and intercept a segment of the noise signal to estimate the noise power W_p .

Step2 : ThefrequencycoarseestimationisobtainedbymodifiedARDalgorithm

Find the solution to $g_l(x) = \frac{|R(p-1)| - W_p}{|R(p)| - W_p}$ by Newton's gradient descent method, yields x_l , and $f_l = (p + x_l)\Delta f$,

Find the solution to $g_r(x) = \frac{|R(p+1)| - W_p}{|R(p)| - W_p}$ by Newton's gradient descent method, yields x_r , and $f_r = (p + x_r)\Delta f$,

Calculate $D(f_l)$, $D(f_r)$, respectively, and compare the magnitudes,

If $|D(f_l)| > |D(f_r)|$, then $x_c = x_l$,

else $x_c = x_r$.

The coarse estimation results are $f_c = (p + x_c)\Delta f$, and the coarse index value is $\hat{m} = p + x_c$.

Step3 : AccuratefrequencyestimatesareobtainedbyiterativeFFTinterpolation forzero – padding

Accurate frequency estimation based on FFT interpolation algorithm.

Set $\hat{\delta}_0 = 0$

Loop: for each i from 1 to Q do

$$\begin{aligned}
X_{\Delta p} &= \sum_{k=0}^{N-1} s(k) e^{-j2\pi k \frac{\hat{m} + \hat{\delta}_{i-1} + \Delta p}{M}}, \quad \Delta p = \pm p = \pm 0.5 \frac{M}{N}, \\
\hat{\delta}_i &= \hat{\delta}_{i-1} + \frac{2N}{M} \text{Re} \left\{ \frac{X_p + X_{-p}}{X_p - X_{-p}} \right\}.
\end{aligned}$$

Step4 : Finally frequency estimation results were obtained

$$\hat{f} = (\hat{m} + \hat{\delta}_Q) \Delta f.$$

4 Algorithm performance analysis

As can be seen from the previous section, the essence of our method for performing the correction based on the coarse estimate of ARD is actually just a correction for the coarse estimate results, so the final performance of this MARD-FFCI algorithm is still determined by the zero-padding-based MFFCI algorithm, and in reference [11], it is clearly stated that the performance limit of the AM algorithm is 1.0147 CRLB, which is already very close to the CRLB, but this theoretical performance is still based on non-padded signals.

Then, the focus of this section will be on how much performance can be achieved by the modified AM algorithm proposed in this paper, and whether it is related to zero-padding. In literature [27], the calculation of the spectral lines of Gaussian white noise based on FFT estimation is presented as follows

$$\limsup_{N \rightarrow \infty} \sup_{\lambda} \frac{|W(\lambda)|^2}{N \ln N} \leq 1. \quad (41)$$

Since we use a signal of length N with an M -point FFT, we can assume that $W(\lambda)$ is in the order of $O(\sqrt{M \ln M})$.

According to Eqs. (38) and (39), we can obtain

$$\beta = \frac{X_p + X_{-p}}{X_p - X_{-p}} = \frac{\left(b \frac{\delta}{\delta - p} + W_p\right) + \left(b \frac{\delta}{\delta - (-p)} + W_{-p}\right)}{\left(b \frac{\delta}{\delta - p} + W_p\right) - \left(b \frac{\delta}{\delta - (-p)} + W_{-p}\right)}. \quad (42)$$

After simplification, the following equation can be obtained

$$\beta = \frac{2\delta + \frac{\delta^2 - p^2}{b\delta} (W_p + W_{-p})}{2p + \frac{\delta^2 - p^2}{b\delta} (W_p - W_{-p})}. \quad (43)$$

$W(\lambda)$ is in the order of $O(\sqrt{M \ln M})$. By the definition of b , we can know that b is in the order of $O(M)$, and then β in the order of $O(M^{-1/2} \sqrt{\ln M})$. Therefore, when N is large, according to the McLaughlin formula, we can approximate Eq. (43) as

$$\beta = \left[2\delta + \frac{\delta^2 - p^2}{b\delta} (W_p + W_{-p})\right] \times \left[2p - \frac{\delta^2 - p^2}{b\delta} (W_p - W_{-p}) + O(M^{-1} \ln M)\right]. \quad (44)$$

Expand Eq. (44) to obtain

$$\begin{aligned}
\beta = & 4\delta p + 2p \frac{\delta^2 - p^2}{b\delta} (W_p + W_{-p}) - 2\delta \frac{\delta^2 - p^2}{b\delta} (W_p - W_{-p}) \\
& - \frac{\delta^2 - p^2}{b\delta} (W_p + W_{-p}) \frac{\delta^2 - p^2}{b\delta} (W_p - W_{-p}) \\
& + 2\delta O(M^{-1} \ln M) + \frac{\delta^2 - p^2}{b\delta} (W_p + W_{-p}) O(M^{-1} \ln M).
\end{aligned} \quad (45)$$

Ignoring the higher order terms that follow, we obtain

$$\beta = 4\delta p + \frac{\delta^2 - p^2}{b\delta} [2p(W_p + W_{-p}) - 2\delta(W_p - W_{-p})] - O(M^{-1} \ln M). \quad (46)$$

In this way, we can find:

$$\begin{aligned}
\hat{\delta} &= \delta - \frac{\beta}{4p} \\
&= -\frac{1}{4p} \frac{\delta^2 - p^2}{b\delta} \times [(2p - 2\delta)\text{Re}(W_p) + (2p + 2\delta)\text{Re}(W_{-p})] - O(M^{-1} \ln M).
\end{aligned} \quad (47)$$

Thus, we can obtain the theoretical variance of the estimated results as

$$\text{var}[\hat{\delta}] = \frac{1}{16p^2} \left(\frac{\delta^2 - p^2}{|b|\delta} \right)^2 \times [(2p - 2\delta)^2 \text{var}(W_p) + (2p + 2\delta)^2 \text{var}(W_{-p})]. \quad (48)$$

As we mentioned in previous section, the noise obeys a Gaussian distribution, so $\text{var}(W_p) = \text{var}(W_{-p}) = \frac{M\sigma^2}{2}$. According to the definition of b , Eq. (47) can be written as:

$$\text{var}[\hat{\delta}] = \frac{1}{16p^2} \left(\frac{\delta^2 - p^2}{\left| \frac{-MA_0 e^{j\theta} (1 + \exp(j2\pi \delta \frac{N}{M}))}{j2\pi \delta} \right| \delta} \right)^2 \times \left[(2p - 2\delta)^2 \frac{M\sigma^2}{2} + (2p + 2\delta)^2 \frac{M\sigma^2}{2} \right]. \quad (49)$$

After simplification, we obtain

$$\begin{aligned}
\text{var}[\hat{\delta}] &= \frac{1}{16p^2} \frac{(\delta^2 - p^2)^2}{M^2 A_0^2 \frac{4\cos^2(\pi \delta \frac{N}{M})}{(2\pi \delta)^2} \delta^2} \times (8p^2 + 8\delta^2) \frac{M\sigma^2}{2} \\
&= \frac{1}{4p^2} \frac{\pi^2 (\delta^2 - p^2)^2}{MA_0^2 \cos^2(\pi \delta \frac{N}{M})} \times (p^2 + \delta^2) \sigma^2.
\end{aligned} \quad (50)$$

According to the previous algorithm definition, we can get $\hat{f} = (\hat{m} + \hat{\delta}_Q) \Delta f$ and the SNR is defined as $\rho = \frac{A_0^2}{\sigma^2}$. If we ignore the effect of iteration for now, then the variance of the frequency estimates is

$$\begin{aligned}\hat{\sigma}_f^2 &= \text{var} \left[\hat{\delta} \frac{f_s}{M} \right] \\ &= \frac{f_s^2}{4M^3 \rho} \frac{\pi^2 (\delta^2 - p^2)^2}{\cos^2 \left(\pi \delta \frac{N}{M} \right)} \times \left(1 + \frac{\delta^2}{p^2} \right).\end{aligned}\quad (51)$$

Although the exact value of the CRLB for the zero-padding signals has not been verified by any paper and kept unknown, we still use $\hat{\sigma}_f^2 / \sigma_f^2$ to analyze the estimation error for unifying the reference forms:

$$\begin{aligned}\frac{\hat{\sigma}_f^2}{\sigma_f^2} &= \frac{\frac{f_s^2}{4M^3 \rho} \frac{\pi^2 (\delta^2 - p^2)^2}{\cos^2 \left(\pi \delta \frac{N}{M} \right)} \times \left(1 + \frac{\delta^2}{p^2} \right)}{\frac{6f_s^2}{(2\pi)^2 \rho M^3}} \\ &= \frac{\pi^4 (\delta^2 - p^2)^2 \times \left(1 + \frac{\delta^2}{p^2} \right)}{6 \cos^2 \left(\frac{\pi \delta}{2p} \right)}.\end{aligned}\quad (52)$$

By simulation and simple proof, it can be found that the monotonicity of the above equation is independent of Δp and the function has the smallest value when $\delta = 0$. We define it as

$$R_0 = \frac{\pi^4}{6} p^4. \quad (53)$$

The theoretical performance analysis shows that the modified AM algorithm is related to N, M , though it is able to be estimated for zero-padding. Since $\Delta p = \pm 0.5 \frac{M}{N}$ is defined in the preceding section and N is less than or equal to M , it can be seen that estimation variance will also be much larger for a small duty-cycle than for a large duty-cycle though the modified interpolation algorithm takes zero-padding into consideration.

5 Algorithm performance simulation

The proposed algorithm aims to perform an accurate frequency estimation for zero-padded Sinusoidal Signal by combining and modifying the two main DFT coefficient-based algorithms. The purpose of the study is to overcome the shortcomings of the traditional interpolation algorithm, which only performs better when the residual frequency error is small, and to improve the performance of the adjacent DFT coefficient-based ratio method. The proposed algorithm will combine the two algorithms with low SNR for zero-padding to achieve higher estimation accuracy.

In this section, data simulation experiments are conducted firstly for each part of the algorithm flow implementation. We analyze the impact of each part on the proposed algorithm and the simulation results of the algorithm for different parameters. Then, the comparison with other exact estimators for no-padding and for zero-padded signals is discussed separately. In each Monte Carlo simulation, we obtain the simulation error as:

$$MSE = \frac{1}{M} \sum_{i=1}^M (\hat{f}_i - f)^2. \quad (54)$$

It is worth noting that scholars has not given the closed-form solution to theoretical CRLB under the zero-padding yet, so the results of comparison in this paper are presented for the CRLB values of non-padded signals. It can be seen from the third section of this paper that the performance of the theoretical modified interpolation algorithm should be related to the percentage of zero-padding. The calculated result is $\frac{\pi^4}{6}p^4$. Substituting M, N , we can obtain

$$R_0 = \frac{\pi^4 0.5^4}{6} \left(\frac{M}{N} \right)^4. \quad (55)$$

Since we assume that it is zero-padding that results in the effect of this correction term, the log AsymptoticCRLB (ACRLB) can be obtained as

$$\begin{aligned} ACRLB &= 10 \lg R_0 \\ &= 10 \lg CRLB + 10 \lg \left(\frac{M}{N} \right)^4 \\ &= 10 \lg CRLB + 40 \lg \frac{M}{N} \end{aligned} \quad (56)$$

5.1 Performance analysis of improved interpolation algorithm

As can be seen in the preceding section, the proposed iterative interpolation frequency estimation algorithm based on ARD is obtained by combining the modified FFCI algorithm after referring to the literature [25]. The ARD algorithm is simple to calculate and uncomplicated to implement, but there are also errors because the DTFT coefficients are calculated by the Newton method, instead of by the derivation of the closed-form solution. Therefore, we drew lessons from the ARD algorithm and performed coarse estimation based on the magnitude ratio method by the spectral lines adjacent to the maximum spectral line, and then take the results as the initial value of the iterative algorithm. The fine estimation did not adopt the ratio algorithm but modified fractional FFT coefficient interpolation iterative algorithm. In this way, not only the defects of the ARD algorithm, which is not accurate and has no theoretical error value, are solved, but also the problem that the interpolation iteration method is sensitive to the coarse estimation is compensated.

This section includes the feasibility analysis of the proposed algorithm and simulations for the FFCI interpolation iterative algorithm by ARD coarse estimation and MBS coarse estimation. The simulations are also for the combination of ARD coarse estimation and unmodified interpolation algorithm. Finally, MARD-FFCI algorithm is proposed.

The algorithm proposed in this paper is for zero-padded signals, which is the focus of this section. The algorithm comparison for non-padded signals will be discussed in later section, which will not be elaborated in this section. The simulation conditions in Fig. 5 are: $f_s = 2048$, total signal length $M = 2048$, sinusoidal signal length $N = 1024$, initial phase random for each simulation, signal frequency $f = (16 + \delta)\Delta f$, and Monte Carlo count is 50,000. In Fig. 5a, $\delta = 0.45$, $\text{SNR} = -20:2:30$; In Fig. 5b, $\text{SNR} = 10\text{dB}$, $\delta = -0.5:0.05:0.5$. The number of iterations of AM algorithm here is 2, and the iterations number of the MARD-FFCI algorithm is also 2. The data of Fig. 5 indicate that the traditional iterative interpolation iterations do not eliminate the effect of residual frequency

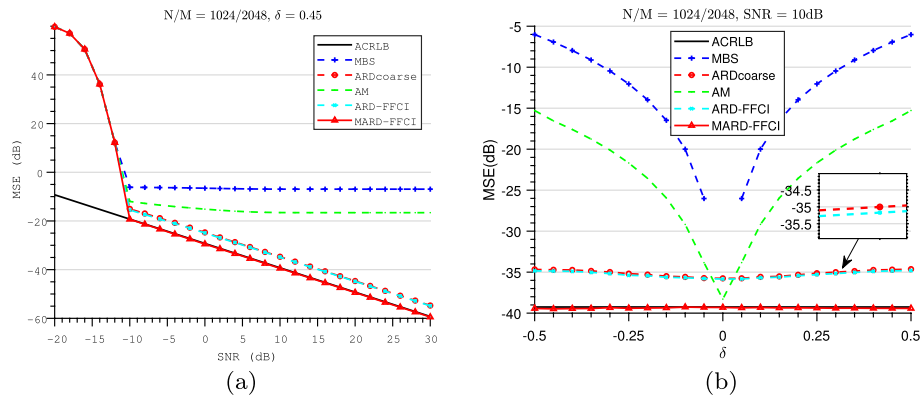


Fig. 5 Analysis of the performance results of the MARD-FFCI algorithm and the components, (a) The relationship between the estimation errors and SNR. The estimation errors are for different rough estimation methods combined with fine estimation methods and for the proposed modified algorithm, when a residual error factor is 0.45. (b) The relationship between estimation errors versus residual errors for different coarse estimation methods combined with fine estimation and for the proposed modified algorithm when SNR is 10 dB

deviations that are not near the zero point, while the ARD coarse estimation, compared with the MBS coarse estimation, can be seen to have a positive effect of correcting deviations for zero-padded signals. But performance does not be improved greatly by the exact estimation if we take the ARD coarse estimation and the interpolation algorithm only. As shown in Fig. 5b, the two algorithm are almost at the same level with an error of about 0.2 dB, while the proposed algorithm in this paper can improve the estimation performance more significantly on the basis of the ARD coarse estimation.

5.2 Simulation of improved interpolation algorithms and common algorithms applied to non-padded signals

This section focuses on the performance comparison of some common algorithms with our proposed algorithm. The algorithms compared in this section include FFCI, MOI—the basic algorithms of the proposed algorithm, and the classical iterative interpolation algorithm AM; The algorithms compared also include the estimation algorithms with better performance which are studied in recent years, and QSE, HAQSE, and ARD algorithm, the algorithms with the best results for zero-padding at present.

The simulation parameters in Fig. 6 are: SNR = -20:30 dB, $f_s = 2048$, FFT points as well as signal length are $N = 1024$, initial phase is random, $f = (16 + \delta)\Delta f$, and Monte Carlo count is 50,000.

Figure. 6 shows simulations for fixed frequency deviation for different SNRs, It can be seen that many current algorithms have good estimation performance for non-padding and smaller frequency residuals, and most of algorithms can provide accurate frequency estimation for sinusoidal signals at SNR above -10 dB. A partial zoom on Fig. 6a shows that the traditional non-iterative fractional interpolation algorithm has a performance differences from the later traditional non-iterative fractional interpolation algorithm, but the differences are in acceptable limits. However, compared to the later algorithms, the traditional fractional Fourier coefficient interpolation algorithm is more sensitive to the residual frequency deviation, that is,

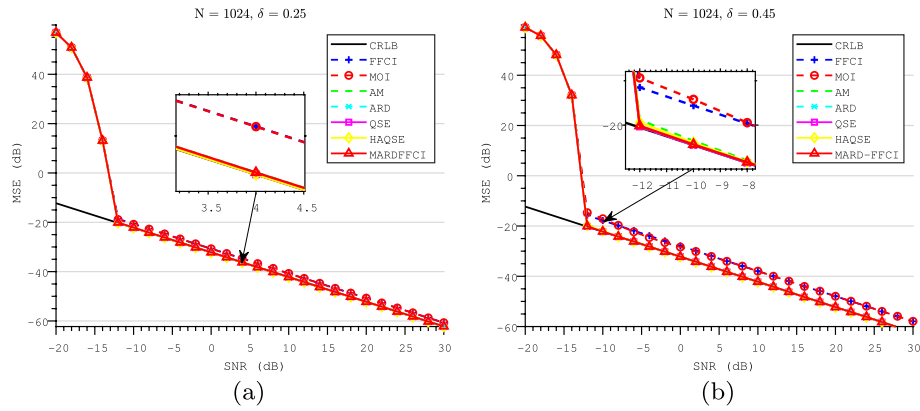


Fig. 6 Comparison of estimation performance results of different algorithms for non-padded signals with CRLB, **a** simulation results of frequency estimation versus SNR for $\delta = 0.25$, **b** simulation results of frequency estimation versus SNR for $\delta = 0.45$

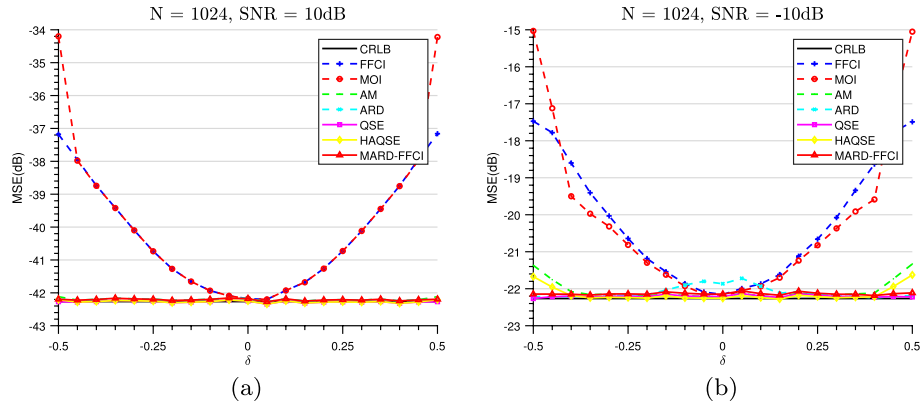


Fig. 7 Simulation results of estimation error versus residual frequency deviation for non-padded signals by different algorithms, **a** simulation error versus residual frequency deviation with $\text{SNR}=10\text{dB}$, **b** simulation error versus residual frequency deviation with $\text{SNR}=-10\text{dB}$

significant performance difference will occur for different values of δ . The obvious difference can be seen when a frequency residual deviation is 0.45. The SNR performance of the algorithm proposed in this paper can achieve similar effects with the known frequency estimation algorithms.

To verify the algorithm performance simulation for different values of δ , the following parameter simulation are performed: $f_s = 2048$, FFT points as well as signal length are $N = 1024$, initial phase is random, $f = (16 + \delta)\Delta f$, and Monte Carlo count is 50,000. From Fig. 7, we can see that most of the current frequency estimation algorithms can achieve relatively smooth and accurate frequency estimation under high SNR conditions, except for the traditional non-iterative frequency domain interpolation algorithm. But, under low SNR conditions, few algorithms can achieve the same smoothness as the proposed algorithm in this paper, which shows that the proposed algorithm has very good estimation performance even under non-padding signal conditions.

5.3 Simulation of improved interpolation algorithms and common algorithms applied to zero-padded signals

To verify the performance of the algorithm proposed in this paper and some other algorithms for zero-padded signals, we performed the simulation and performance analysis of the algorithms for zero-padded signals, in which the parameters are the same as the preceding sections, except that this simulation are for the zero-padded signals with different duty cycles. The simulation results are shown in Fig. 8.

From Fig. 8, it can be seen that most of the current frequency estimation algorithms are not effective for zero-padded signals, while the MARD-FFCI algorithm can perform effective estimation for zero-padded signals. Moreover, the ARD algorithm can perform zero-padded signal estimation to some extent but the estimation performance is better under the condition of higher duty cycle. When the duty cycle of the signal decreases, the gap with the algorithm proposed in this paper will show obviously.

The results of accurate frequency estimation for zero-padded signals at high SNR and low SNR, respectively, are shown in Fig. 9. The basic simulation parameters are the same as ones in preceding sections. From Fig. 9, we can see that the MARD-FFCI algorithm can estimate the frequency values very effectively in both low and high SNR conditions. It can be seen also that the error between the estimated MSE and the nonzero-padded

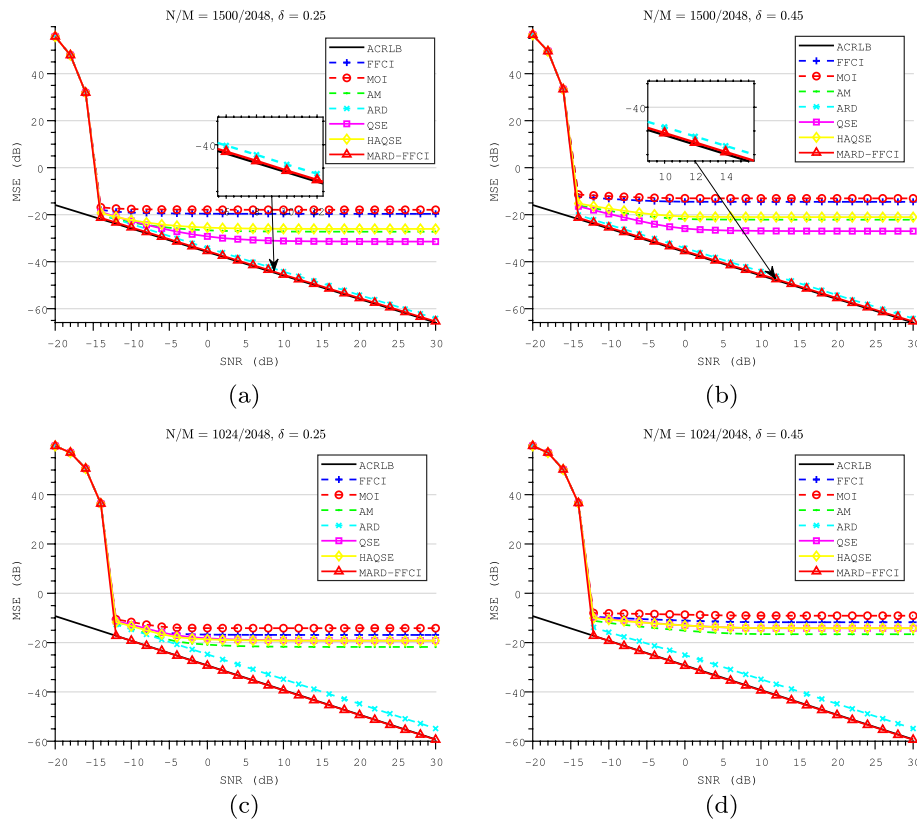


Fig. 8 Estimation performance results of different algorithms for zero-padded signals versus SNRs, **a** simulation results of frequency estimation versus SNRs for $\delta = 0.25$ with N/M of 1500/2048, **b** simulation results of frequency estimation versus SNRs for $\delta = 0.45$ N/M of 1500/2048, **c** simulation results of frequency estimation versus SNRs for $\delta = 0.25$ N/M of 1024/2048, **d** simulation results of frequency estimation versus SNRs for $\delta = 0.45$ N/M of 1024/2048

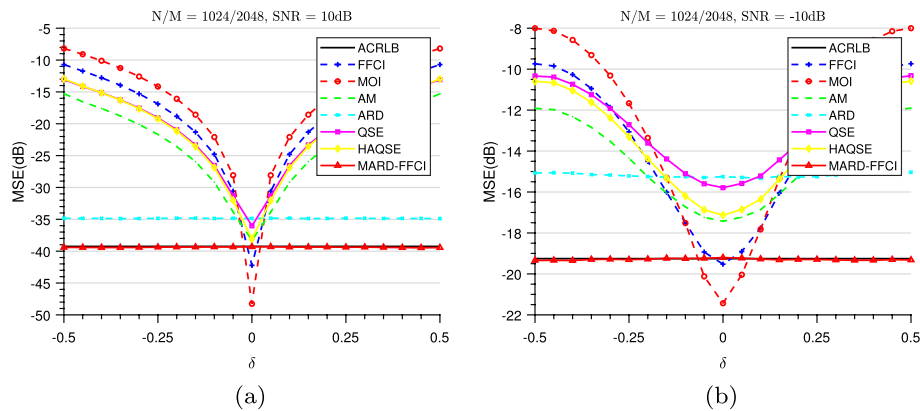


Fig. 9 Estimation performance results of different algorithms for zero-padded signals versus residual error, **a** simulation results of frequency estimation versus residual frequency error for $\text{SNR} = 10\text{ dB}$, **b** simulation results of frequency estimation versus residual frequency error for $\text{SNR} = -10\text{ dB}$

signals is in agreement with the theoretical calculation. In contrast, other high-precision estimation algorithms are basically invalid for zero-padding signals because of the defects of sensitivity to residuals. While another ARD algorithm for zero-padded signals shows an obvious performance inferiority with the algorithm proposed in this paper. Moreover, the performance of ARD algorithm is not very stable under the condition of low SNR, which is more different from the algorithm proposed in this paper.

In summary, the MARD-FFCI algorithm proposed in this paper shows obvious advantages in the simulation, not only in the zero-padding case, but also get same performance as the comparison algorithm in the nonzero-padding case, and what is more valuable is that the algorithm is also consistent with the theoretical results obtained in this paper, so it has good prospects for application.

6 Conclusions

Accurate frequency estimation of single-frequency signals is a classical problem in signal processing. Few studies have been reported on frequency estimation of signals for zero-padding signals. The traditional interpolated frequency estimation usually adopts DFT or DTFT sample values to approximate the true frequency, but this mode is more demanding for coarse estimation which iterative computation has to be adopted. The disadvantages are the need for large amount of computation and no effective iterative accurate frequency estimation algorithms for zero-padded signals. To address this problem, this paper proposes an estimation algorithm based on coarse estimation of the frequency ratio and on modified fractional Fourier coefficient interpolation. In order to get an accurate coarse estimation, a modified frequency coarse estimation algorithm on Fourier coefficient ratio is proposed for zero-padded signals. In the process of fine estimation, a fractional Fourier coefficient interpolation algorithm for zero-padded signals is also suggested, by which good results can be achieved without iteration. This algorithm also allows performance improvement in iteration. Another advantage is that the algorithm is applicable not only for zero-padded signals but also for non-padded signals. The last advantage is that it is characterized by low fluctuation for different frequency residuals. To our knowledge, the proposed algorithm is the best accurate frequency

estimator for single frequency zero-padded signals, which is verified by extensive computer simulations.

Acknowledgements

The authors are grateful to the anonymous reviewers and for the research funding support.

Author Contributions

Conceptualization was contributed by LL and JY, methodology was contributed by LL, software was contributed by LL, validation was contributed by JY, XH and WG, formal analysis was contributed by LL, writing—original draft preparation was contributed by LL, writing—review and editing was contributed by XH, visualization was contributed by XH, supervision was contributed by JY, project administration was contributed by XH, funding acquisition was contributed by JY. All authors discussed the results, contributed to the manuscript, and approved the final manuscript.

Funding

This research was funded by National Key R & D Program of China (2021YFC2801200) and National Natural Science Foundation of China (62127801).

Availability of data and materials

Please contact author for data requests.

Declarations

Competing interests

The authors declare that they have no competing interests.

Received: 6 January 2023 Accepted: 22 May 2023

Published online: 02 June 2023

References

1. J. Zhang, L. Tang, A. Mingotti, L. Peretto, H. Wen, Analysis of white noise on power frequency estimation by DFT-based frequency shifting and filtering algorithm. *IEEE Trans. Instrum. Meas.* **69**, 4125–4133 (2020)
2. O.I. Khalaf, G.M. Abdulsahib, Frequency estimation by the method of minimum mean squared error and p-value distributed in the wireless sensor network. *J. Inf. Sci. Eng.* **35**, 1099–1112 (2019)
3. D.A. Abraham, Underwater acoustic signal processing. *Modern Acoust. Signal Process.* (2019)
4. R. Schmidt, R.O. Schmidt, Multiple emitter location and signal parameter estimation. *IEEE Trans. Antennas Propag.* **34**(3), 276–280 (1986)
5. R. Roy, T. Kailath, Esprit - estimation of signal parameters via rotational invariance techniques. *IEEE Trans. Acoust. Speech Signal Process.* **37**(7), 984–995 (1989)
6. D.C. Rife, G. Vincent, Use of the discrete Fourier transform in the measurement of frequencies and levels of tones. *Bell Syst. Tech. J.* **49**(2), 197–228 (1970)
7. D. Rife, R. Boorstyn, Single tone parameter estimation from discrete-time observations. *IEEE Trans. Inf. Theory* **20**(5), 591–598 (1974)
8. G.-Q. Qi, X.-L. Jia, Accuracy analysis of frequency estimation of sinusoid based on interpolated FFT. *ACTA Electron. Sinica* **32**(4), 625 (2004)
9. X.D. Wang, Y. Liu, Z.M. Deng, Modified rife algorithm for frequency estimation of sinusoid and implementation in FPGA. *Syst. Eng. Electron.* (2008)
10. E. Aboutanios, Frequency estimation for low earth orbit satellites. PhD thesis (2002)
11. E. Aboutanios, B. Mulgrew, Iterative frequency estimation by interpolation on Fourier coefficients. *IEEE Trans. Signal Process.* **53**(4), 1237–1242 (2005)
12. Y. Li, J. Zhao, J. Li, X. Lei, Y. Fu, A new algorithm for frequency estimation based on frequency searching. In: 2016 IEEE International Conference on Digital Signal Processing (DSP), pp 223–226 (2016). IEEE
13. D. Belega, D. Petri, Frequency estimation by two-or three-point interpolated Fourier algorithms based on cosine windows. *Signal Process.* **117**, 115–125 (2015)
14. S. Ye, J. Sun, E. Aboutanios, On the estimation of the parameters of a real sinusoid in noise. *IEEE Signal Process. Lett.* **24**(5), 638–642 (2017)
15. A. Serbes, Fast and efficient sinusoidal frequency estimation by using the DFT coefficients. *IEEE Trans. Commun.* **67**(3), 2333–2342 (2018)
16. J.-R. Liao, S. Lo, Analytical solutions for frequency estimators by interpolation of DFT coefficients. *Signal Process.* **100**, 93–100 (2014)
17. Ç. Candan, A method for fine resolution frequency estimation from three DFT samples. *IEEE Signal Process. Lett.* **18**(6), 351–354 (2011)
18. Ç. Candan, Analysis and further improvement of fine resolution frequency estimation method from three DFT samples. *IEEE Signal Process. Lett.* **20**(9), 913–916 (2013)
19. Ç. Candan, U. Çelebi, Frequency estimation of a single real-valued sinusoid: an invariant function approach. *Signal Process.* **185**, 108098 (2021)
20. A.A. D'Amico, M. Morelli, M. Moretti, Frequency estimation by interpolation of two Fourier coefficients: Cramér-rao bound and maximum likelihood solution. *IEEE Trans. Commun.* **70**(10), 6819–6831 (2022)

21. Y. Cui, W. Gang, A noniterative frequency estimator with rational combination of three spectrum lines. *IEEE Trans. Signal Process.* **59**(10), 5065–5070 (2011)
22. L. Fan, G. Qi, J. Xing, J. Jin, J. Liu, Z. Wang, Accurate frequency estimator of sinusoid based on interpolation of FFT and DTFT. *IEEE Access* **8**, 44373–44380 (2020)
23. A. Carboni, A. Ferrero, A Fourier transform-based frequency estimation algorithm. *IEEE Trans. Instrum. Meas.* **67**(7), 1722–1728 (2018)
24. X. Jinzhi, S. Qing, C. Wei, A novel single tone frequency estimation by interpolation using dft samples with zero-padding. In: 2016 IEEE 13th International Conference on Signal Processing (ICSP), pp 277–281 (2016). IEEE
25. Y. Zhang, Y. Xie, X. Li, X.P. Zhang, J. Zhou, Frequency estimation for zero-padded signal based on the amplitude ratio of two DFT samples. *IEEE Trans. Signal Process.* **69**, 6504–6514 (2021)
26. S.K. Sengijpta, Fundamentals of statistical signal processing: estimation theory. *Technometrics* **37**(4), 465–466 (1993)
27. B. Porat, Digital processing of random signals: theory and methods (2008)

Publisher's Note

Springer Nature remains neutral with regard to jurisdictional claims in published maps and institutional affiliations.

Submit your manuscript to a SpringerOpen[®] journal and benefit from:

- Convenient online submission
- Rigorous peer review
- Open access: articles freely available online
- High visibility within the field
- Retaining the copyright to your article

Submit your next manuscript at ► [springeropen.com](https://www.springeropen.com)
